Foraging theory predicts predator–prey energy fluxes

U. Brose[1,2]*, R. B. Ehnes[1], B. C. Rall[1], O. Vucic-Pestic[1], E. L. Berlow[2,3] and S. Scheu[1]

[1]*Darmstadt University of Technology, Department of Biology, Schnittspahnstr. 10, 64287 Darmstadt, Germany;*
[2]*Pacific Ecoinformatics and Computational Ecology Laboratory, Berkeley, CA 94703, USA; and* [3]*University of California, Merced, Sierra Nevada Research Institute, Wawona Station, Yosemite National Park, CA 95389, USA*

Summary

1. In natural communities, populations are linked by feeding interactions that make up complex food webs. The stability of these complex networks is critically dependent on the distribution of energy fluxes across these feeding links.

2. In laboratory experiments with predatory beetles and spiders, we studied the allometric scaling (body-mass dependence) of metabolism and per capita consumption at the level of predator individuals and per link energy fluxes at the level of feeding links.

3. Despite clear power-law scaling of the metabolic and per capita consumption rates with predator body mass, the per link predation rates on individual prey followed hump-shaped relationships with the predator–prey body mass ratios. These results contrast with the current metabolic paradigm, and find better support in foraging theory.

4. This suggests that per link energy fluxes from prey populations to predator individuals peak at intermediate body mass ratios, and total energy fluxes from prey to predator populations decrease monotonically with predator and prey mass. Surprisingly, contrary to predictions of metabolic models, this suggests that for any prey species, the per link and total energy fluxes to its largest predators are smaller than those to predators of intermediate body size.

5. An integration of metabolic and foraging theory may enable a quantitative and predictive understanding of energy flux distributions in natural food webs.

Key-words: allometric scaling, biological control, body size, food webs, ingestion rates, interaction strength, metabolic theory, top-down control

Introduction

Natural ecosystems comprise a large number of species engaging in a vast number of predator–prey interactions of variable strength (Berlow *et al*. 2004; Wootton & Emmerson 2005). Two categories of interaction strength most commonly studied include (1) the magnitude of energy flowing from prey to predator, or predator consumption rates; and (2) the change in abundance of one species given a change in abundance of another, or the dynamic coupling of two species. Both measures provide insight into the stability of complex food webs (Brose, Williams & Martinez 2006b; Montoya, Pimm & Sole 2006; Navarrete & Berlow 2006; Neutel *et al*. 2007; Otto, Rall & Brose 2007; Rall, Guill & Brose 2008). Thus a critical step for moving beyond descriptive, community-specific approaches in ecology is to uncover general principles that determine interaction strengths (Berlow *et al*. 2004; Brose, Berlow & Martinez 2005; Wootton & Emmerson 2005). While not always directly related, high consumption rates (high

energy fluxes) can establish the potential for strong dynamic coupling between two species (Bascompte, Melian & Sala 2005; Brose *et al*. 2005). Here we focus on general principles that determine energy fluxes, because recent allometric models based on metabolic scaling theory (Brown *et al*. 2004) have proposed that predator consumption rates follow a power-law increase with predator body mass (Yodzis & Innes 1992; Emmerson & Raffaelli 2004; Reuman & Cohen 2005; Wootton *et al*. 2005). The elegant simplicity and empirical tractability of this theory has led to its recent widespread application in theoretical studies (McCann, Hastings & Huxel 1998; Emmerson & Raffaelli 2004; Williams & Martinez 2004; Brose *et al*. 2006b).

By defining physiological constraints, metabolic theory predicts the per capita (per individual) and total consumption rates necessary to sustain a population. However, being based only on predator body masses, this approach cannot distinguish the energy fluxes among the individual feeding links of generalist predators (hereafter, per link fluxes). It thus predicts per link fluxes by distributing per capita consumption rates equally across the feeding links. In contrast, foraging theory

uses traits of the prey species, such as average body masses (where the average is an evolutionarily stable mean over the individuals of a population), to predict how behavioural aspects of predator–prey interactions determine the relative strength of these feeding links while ignoring the overall energy flux at the level of predator individuals. Here we propose a framework that integrates metabolic theory at the levels of predator individuals (per capita) with foraging theory at the level of feeding interactions (per link). Our focus on predator–prey energy fluxes complements recent analyses of how allometric foraging models predict food-web topology (Beckerman, Petchey & Warren 2006). We first introduce the models, then test their predictions using laboratory data on metabolism and consumption of arthropods. Macroecological abundance–mass relationships scale-up these predictions to natural communities with variance in predator and prey abundance.

MODELS

Per capita metabolism and consumption

At the level of individuals, metabolic theory predicts that the metabolic rates of species i, I_i [J s^{-1}] scale with body mass, M_i (g) as:

$$I_i = I_0 M_i^a \qquad \text{eqn 1}$$

where I_0 and a are constants (Brown *et al.* 2004). Moreover, it predicts that per capita consumption rates of consumer individuals of species i, C_i [J s^{-1}], follow a similar mass-dependence to the metabolic rates:

$$C_i = C_0 M_i^b \qquad \text{eqn 2}$$

where C_0 and b are constants (Carbone, Teacher & Rowcliffe 2007).

Per link consumption

Direct application of this per capita relationship (equation 2) to individual feeding interactions between predator i and prey j yield per link consumption rates, K_{ij} [J s^{-1}]:

$$K_{ij} = K_0 M_i^b \qquad \text{eqn 3}$$

where K_0 is a constant and

$$C_i = \sum_j K_{ij}$$

(Yodzis & Innes 1992; Brown *et al.* 2004). This 'metabolic model' predicts energy fluxes through individual links by distributing the predator's per capita consumption rate equally across its feeding links.

In contrast, foraging theory suggests that per link predation rates P_{ij} [ind s^{-1}] (the number of individuals of prey j consumed per individual of predator i) follow a hump-shaped relationship with predator–prey body-mass ratios $R_{ij} = M_i/M_j$:

$$P_{ij} = P_{\max} \left[\frac{R_{ij}}{R_{\max}} \exp\left(1 - \frac{R_{ij}}{R_{\max}} \right) \right]^\gamma \qquad \text{eqn 4}$$

where $P_{\max}$ [ind s^{-1}] is the maximum predation rate, $R_{\max}$ is the body-mass ratio at which this maximum is achieved, and γ is a scaling constant (Wilson 1975; Persson *et al.* 1998; Wahlstrom *et al.* 2000; Bystrom *et al.* 2003; Aljetlawi, Sparrevik & Leonardsson 2004; Finstad, Ugedal & Berg 2006). This phenomenological foraging model describes (1) predation rates increasing with body mass ratios when predators are small relative to their prey ($R_{ij} < R_{\max}$), which is explained by an increasing ability of the predator to subdue and handle prey; and (2) predation rates decreasing with body mass ratios when predators are large relative to their prey ($R_{ij} > R_{\max}$), which results from a decreasing detectability and catchability of smaller prey (Persson *et al.* 1998; Aljetlawi *et al.* 2004).

Macroecological energy fluxes

The metabolic model (equation 3) and the foraging model (equation 4) predict laboratory energy fluxes at a fixed abundance, N_j' [ind]. This implies similar laboratory encounter rates for each prey: E_{ij}'[ind s^{-1}] $= E_0' N_j'$, where E_0' and N_j' are constants that are independent of body mass. In natural communities, however, field encounter rates, E_{ij} [ind s^{-1}] $= E_0 N_j$ depend on field prey abundance, N_j [ind] (Emmerson, Montoya & Woodward 2005) that scales with body mass as:

$$N_j = N_0 M_J^{-c} \qquad \text{eqn 5}$$

where N_0 and c are macroecological constants and often $c \approx 0.75$ (Brown *et al.* 2004; Meehan 2006). Synthesizing either the metabolic model or the foraging model with this macroecological abundance–mass relationship scales up predictions from laboratory to field conditions. The per capita energy flux, F_{ij} [J s^{-1}], through the link from prey population j to an individual of predator population i, can be derived under the metabolic model by normalizing the per link consumption rates (equation 3) by the laboratory encounter rates, E_{ij}', and multiplying them with field encounter rates, E_{ij}:

$$\begin{aligned} F_{ij} &= K_{ij} E_{ij}'^{-1} E_{ij} = K_{ij} E_0'^{-1} N_j'^{-1} E_0 N_j \\ &= E_0'^{-1} E_0 N_0 K_0 N_j'^{-1} M_i^b M_j^{-c} \end{aligned} \qquad \text{eqn 6a}$$

This approach distributes per capita consumption rates across feeding links using encounter rates that apply to averages over individuals within populations, while ignoring differences among individuals. Under the foraging model (equation 4), F_{ij} [J s^{-1}] is equal to predation rates, P_{ij} [ind s^{-1}] divided by the laboratory encounter rate, E_{ij}', and multiplied by the field encounter rate, E_{ij}, and prey energy content [the product of prey mass, M_j [g ind^{-1}] and the energy content per wet mass ε [J g^{-1}]]:

$$\begin{aligned} F_{ij} &= P_{ij} E_{ij}'^{-1} E_{ij} \varepsilon M_j = P_{ij} E_0'^{-1} N_j'^{-1} E_0 N_j \varepsilon M_j \\ &= E_0'^{-1} N_j'^{-1} E_0 N_0 \varepsilon P_{ij} M_j^{1-c} \end{aligned} \qquad \text{eqn 6b}$$

The total energy flux from prey population j to predator population i, T_{ij} [J s^{-1}], is defined as the product of the per capita energy flux (equation 6a or b) and predator abundance, $N_i (N_i = N_0 M_i^{-c})$, which yields:

$$T_{ij} = E_0'^{-1} E_0 K_0 N_0^2 N_j'^{-1} M_i^{b-c} M_j^{-c} \qquad \text{eqn 7a}$$

$$T_{ij} = E_0'^{-1} N_j'^{-1} E_0 N_0^2 \varepsilon P_{ij} M_i^{-c} M_j^{1-c} \qquad \text{eqn 7b}$$

under the metabolic (equation 7a) and foraging (equation 7b) model, respectively.

Methods

We used ground-dwelling beetles and spiders to test these model predictions in laboratory experiments. Pitfall trapping yielded 16 carabid and staphylinid beetle species (*Abax ovalis*, *Abax parallelepipedus*, *Calathus melanocephalus*, *Calathus piceus*, *Carabus auratus*, *Harpalus affinis*, *Nebria brevicollis*, *Notiophilus biguttatus*, *Notiophilus laticollis*, *Ocypus olens*, *Philonthus fuscipennis*, *Platynus dorsalis*, *Poecilus versicolor*, *Pseudophonus rufipes*, *Pterostichus melanarius*, *Pterostichus oblongopunctatus*) and 10 lycosid, pisaurid and salticid spider species (*Alopecosa* sp. juv. I, *Alopecosa* sp. juv. II, *Alopecosa cuneata*, *Pardosa lugubris*, *Pardosa palustris*, *Pirata piraticus*, *Pirata latitans*, *Pisaura mirabilis*, *Salticus scenicus*, *Trochosa terricola*; for authorities see Brohmer 2006). The juveniles of *Alopecosa* sp. were considered as trophic species as they vary from adults in their prey spectrum. We used only adult females of the other spider species. The species chosen are common epigeic predators in central Europe.

All experiments were carried out under controlled laboratory conditions (12 h light per day, 15 °C). We measured the basal metabolic rates of six individuals of each species with an automated electrolytic microrespirometer (Scheu 1992). We converted the measured O$_2$ fluxes (ml O$_2$ s^{-1}) per spider individual into energetic equivalents (J s^{-1}) by assuming that 1 ml O$_2$ equals 20·1 J. Prior to the consumption experiments, the predator species were fed and then starved for 5 days. All individuals were weighed before and after the experiments on a precision scale. We used the average of these weights throughout all analyses. We used collembolans (*Heteromurus nitidus*) and crickets (*Gryllus sigillatus*) as prey for the spiders, and fruit flies (*Drosophila hydei*) and fly larvae (*Lucilia caesar*) as prey for the beetles, which yielded a total of 32 and 20 predator–prey interactions for beetles and spiders, respectively. We studied predation by placing one predator individual in each arena (0·2 × 0·2 m), in which 2·35 g dry moss (*Polytrichum formosum*) was evenly dispersed as habitat structure. The moss was dried for 4 days at 60 °C to exclude other animals, and was moisturized prior to the experiments. In each experimental replicate, one predator individual and 30 individuals of one prey species (initial prey density N_i) were placed in an arena, and we counted the number of prey that remained after 24 h (final prey density N_e). We used eight replicates per predator–prey combination, and calculated the energy fluxes for each replicate (K_{ij} in equation 3) by multiplying the number of prey individuals consumed ($N_c = N_i - N_e$) by the average weight of the prey individuals (g) and the energy content per mg prey wet mass (7 J g^{-1}) (Peters 1983). The use of this general energy content per mg wet mass ignores taxon-specific variation in energy density due to difference in stoichiometry. Given that most of the variation in predator–prey body mass ratios was caused by variance in predator body masses, this generalization appears to cause a relatively small error in energy contents. The predation rates (P_{ij} in equation 4)

equalled the number of prey individuals consumed per individual predator. Control treatments without predators exhibited similar prey densities at the beginning and end of the experiment, suggesting that any decline in prey density in predator enclosures was due to consumption rather than natural mortality. The per capita consumption rates of the predator species (C_i in equation 2) were calculated under the assumptions that the predators encounter and attack their prey by chance, and we averaged the independently measured per link consumption rates of the two prey populations [$j = 1, 2$; $C_i = (K_{i1} + K_{i2})/2$ or $C_i = K_{ij}$ if only j is consumed].

We calculated the averages of the metabolic rate, the per capita consumption rate and the body mass for each predator species, and the averages of the predation rate, per link consumption rate and body mass ratio for each predator–prey interaction. The relationships between (1) average metabolic rate and average predator body mass; (2) average per capita consumption rate and average predator body mass; (3) average per link consumption rate and average predator body mass; and (4) average predation rate and average predator–prey body mass ratio were all analysed by nonlinear least-squares regressions.

Results

PER CAPITA METABOLISM AND CONSUMPTION

The metabolic rates exhibited a power-law increase with the average body mass of the species, but the exponent of the relationship was higher for beetles ($a = 0·76 \pm 0·07$; mean $\pm$ SE, Fig. 1a) than for spiders ($a = 0·43 \pm 0·07$; Fig. 1b). The per
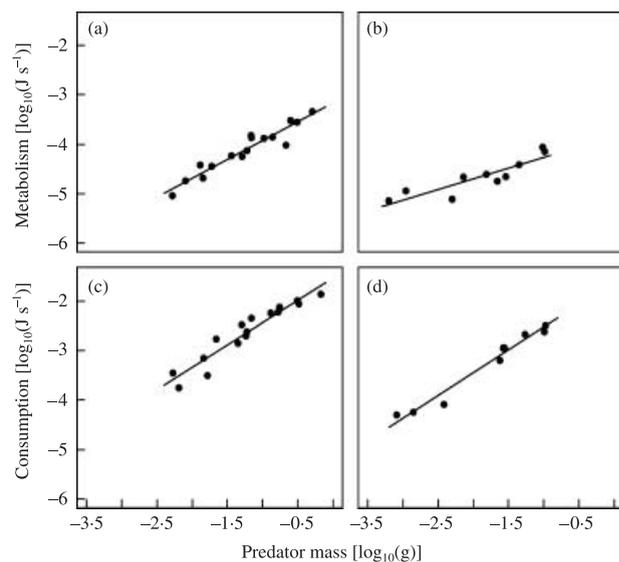

Fig. 1. Laboratory measurements at the species level: metabolism, (a) beetles; (b) spiders) [log$_{10}$ (J s^{-1})] and per capita consumption, (c) beetles; (d) spiders [log$_{10}$ (J s^{-1})] depending on predator body mass (log$_{10}$ g). Fitted model parameters ($\pm$ SE). (a) Equation 1: $a = 0·76 \pm 0·06$; log$_{10} I_0 = -3·17 \pm 0·09$; $r^2 = 0·91$; $P < 0·0001$; $n = 16$; (b) equation 1: $a = 0·43 \pm 0·07$; log$_{10} I_0 = -3·84 \pm 0·16$; $r^2 = 0·8$; $P < 0·001$; $n = 10$; (c) equation 2: $b = 0·9 \pm 0·08$; log$_{10} C_0 = -1·54 \pm 0·1$; $r^2 = 0·91$; $P < 0·0001$; $n = 16$; (d) equation 2: $b = 0·92 \pm 0·06$; log$_{10} C_0 = -1·6 \pm 0·11$; $r^2 = 0·97$; $P < 0·001$; $n = 10$. Predator individuals were the same in upper (a,b) and lower (c,d) panels, but their body masses were slightly heavier in the lower panels because we averaged their masses before and after the feeding experiments.
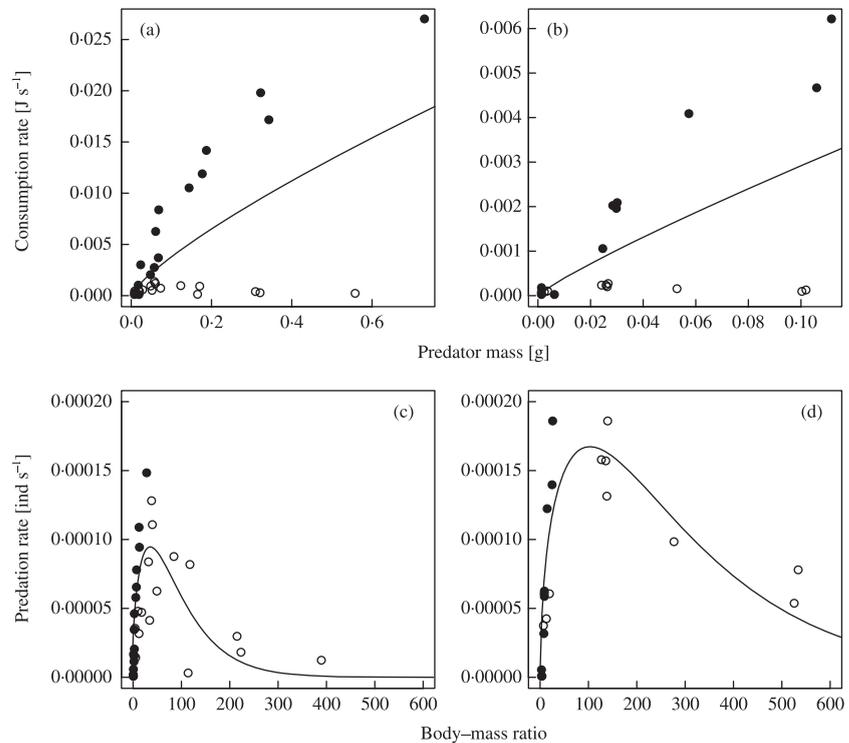
Fig. 2. Laboratory measurements at the level of feeding links: per link consumption rates [$J s^{-1}$] depending on predator body mass (g), (a) beetles; (b) spiders and predation rates (ind s^{-1}) depending on predator–prey body mass ratios, (c) beetles; (d) spiders. Fitted model parameters ($\pm$ SE): metabolic model (equation 3) for (a) beetles ($b = 0.78 \pm 0.22$; $K_0 = 0.02 \pm 0.01$; $r^2 = 0.39$; $n = 32$); (b) spiders ($b = 0.87 \pm 0.42$; $K_0 = 0.02 \pm 0.02$; $r^2 = 0.36$; $n = 20$); foraging model (equation 4) for (c) beetles ($P_{max} = 9.46 \times 10^{-5} \pm 9.59 \times 10^{-6}$; $R_{max} = 38.1 \pm 6.17$; $\alpha = 0.68 \pm 0.16$; $r^2 = 0.6$; $n = 32$); (d) spiders ($P_{max} = 1.67 \times 10^{-4} \pm 1.45 \times 10^{-5}$; $R_{max} = 103.1 \pm 14.47$; $\alpha = 0.54 \pm 0.1$; $r^2 = 0.78$; $n = 20$). Symbols indicate large prey (closed circles) and small prey (open circles).

capita consumption rates also followed a power-law relationship with the average body mass, but the slopes were steeper (Fig. 1c,d).

PER LINK CONSUMPTION

At the level of feeding links, the metabolic model (equation 3) gave a poor fit to the per link consumption rate data for beetles (Fig. 2a, $r^2 = 0.39$) and spiders (Fig. 2b, $r^2 = 0.36$). Interestingly, the per link consumption rates of large predators were higher than predicted by the metabolic model when they consumed the larger of the two prey species (fly larvae for beetles; crickets for spiders; Fig. 2a,b), and were lower than predicted when they consumed the smaller of the two prey species (fruit flies for beetles; collembolans for spiders; Fig. 2a,b). The hump-shaped foraging model (equation 4) explained a much higher fraction of the variation in predation rates of beetles (Fig. 2c, $r^2 = 0.60$) and spiders (Fig. 2d, $r^2 = 0.78$). The maximum predation rates were reached at intermediate body mass ratios of $R_{max} = 38.1 \pm 6.2$ and $R_{max} = 103.1 \pm 14.5$ (mean $\pm$ SE) for beetles and spiders, respectively. Observations during the experiments suggest that predation was limited by the relatively long time needed to subdue and handle the prey at low body mass ratios. At high body mass ratios, predation was limited by the high escape efficiencies of prey species due to fast reaction times and their use of small refuges in the moss vegetation.

MACROECOLOGICAL ENERGY FLUXES

Synthesizing macroecological abundance–mass relationships with the metabolic model (equation 6a) and the foraging model (equation 6b) yields predictions on per capita energy fluxes from a prey population to a predator individual with respect to predator and prey mass (Fig. 3a,b). Due to assumed constants (see Fig. 3 legend) the predicted fluxes should be interpreted only qualitatively. The predictions are based on the measured laboratory per link consumption and predation rates for beetles (Fig. 2a,c), but calculations based on the results for spiders yield qualitatively identical predictions (results not shown). The metabolic model predicts a continuous increase in per capita energy fluxes with increasing predator mass and decreasing prey mass (Fig. 3a). In contrast, the foraging model predicts a hump-shaped relationship between per capita energy fluxes and predator masses, where the hump increases with prey mass (Fig. 3b).

Multiplying per capita energy fluxes (Fig. 3a,b) with predator abundances yields total energy fluxes between prey and predator populations. The metabolic model (equation 7a) predicts that the total energy fluxes increase with increasing predator mass and decreasing prey mass (Fig. 3c). The highest fluxes should thus occur between the smallest prey and the largest predators. In contrast, the foraging model (equation 7b) predicts that the highest fluxes should occur between the smallest predators and the smallest prey species (Fig. 3d).

Discussion

At the species level, we found a three-quarter power-law scaling of the metabolic rates with body masses for beetles, which corroborates metabolic theory (Brown *et al.* 2004). Consistent with prior findings (Foelix 1996), the respiration rates of spiders were lower than those of beetles. Surprisingly, however, we found a much weaker increase in spider metabolism
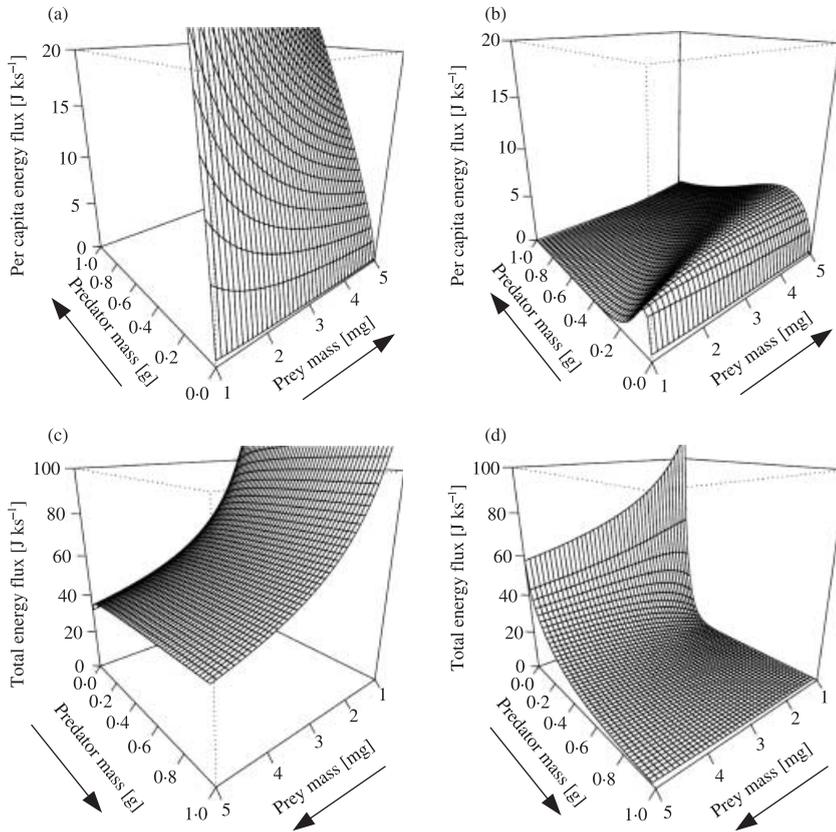
Fig. 3. Per capita (a,b: from a prey population to a predator individual) and total (c,d: from a prey population to a predator population) energy flux as predicted by the synthetic models combining macroecological abundance–mass relationships with the metabolic model: (a) equation 6a; (c) equation 7a; or the foraging model: (b) equation 6b; (d) equation 7b, depending on predator (g) and prey body mass (mg). Calculations are based on per link consumption rates (a,c, see Fig. 2a) or predation rates (b,d, see Fig. 2c) and assumed constants: $E_0' = E_0 = N_0 = 1$; $N_j' = 30$; $\varepsilon = 7$; $c = 0.75$. Thus energy flux values should be interpreted only qualitatively. $k_s = 10^3$ s.

with body mass than predicted by the metabolic theory. Potential explanations for this discrepancy include that (1) the relative contribution of metabolically active tissue to total body mass of small spiders might exceed that in large spiders due to different rates of excretion-storage in their skins (Foelix 1996); and (2) spider metabolism might be limited by factors other than the efficiency of their physiological transport networks (van der Meer 2006). Corroborating metabolic theory, our data illustrate that the per capita consumption rates of both predator groups follow a power-law increase with body mass and exceed the metabolic loss, thus enabling the persistence of the predators.

While each predator's metabolic rate and total consumption were well predicted by power-law functions of predator body mass, the energy fluxes along individual predator–prey links were not. When predator–prey body mass ratios exceeded a threshold (R_{max}), the energy fluxes were limited by a decreasing success rate of the predator attacks due to a higher escape efficiency of the prey. Without the constraints posed by limited attack success, the metabolic model predicts a much stronger increase in energy flux with prey abundance. Interestingly, the two predator groups in our study represent profoundly different feeding strategies: spiders are mainly day-active, optically oriented predators, whereas beetles are mainly nocturnal, tactile and olfactory predators. However, the hump-shaped relationship between predation rates and body mass ratios found for both predator groups was well predicted by a foraging model, which is consistent with

prior studies in aquatic ecosystems (Wahlstrom *et al.* 2000; Bystrom *et al.* 2003; Aljetlawi *et al.* 2004; Finstad *et al.* 2006). While these studies addressed predation rates in size-structured predator–prey interactions with respect to the body masses of individuals, we studied predation rates as a function of the average masses of predator and prey populations. The foraging model used here and in related studies (Wahlstrom *et al.* 2000; Aljetlawi *et al.* 2004) is phenomenological, and the hump-shaped relationship is fit equally well by two power-laws ($P_{ij} \approx R^\phi$ if $R \leq R_{max}$; $P_{ij} \approx R^{-\eta}$ if $R > R_{max}$). However, independent of the choice of model, the broad generality of this hump-shaped relationship across ecosystem types and predator groups suggests that metabolic energy-flux models (Peters 1983; Emmerson *et al.* 2004; Reuman & Cohen 2005) that do not account for this relationship may seriously overestimate per capita energy fluxes between large predators and small prey. Moreover, the hump-shaped relationship between predation rates and predator–prey body mass ratios contrasts classic population dynamic models using power-law per link consumption rates (Yodzis *et al.* 1992), whereas it corroborates recent approaches with unimodal predation rates (Loeuille & Loreau 2005; Weitz & Levin 2006). These patterns suggest that, all else being equal, the dynamic coupling between large predators and small prey may generally be weaker than predicted by a simple metabolic model. As general principles that govern energy flux may be more tractable than those that determine the population dynamics of species interaction strengths, it is critical to explore more thoroughly how and

when consumer foraging patterns can predict the dynamic consequences of a change in consumer abundance (Schmitz 2007).

Some caveats should be mentioned. First, all laboratory experiments were carried out with simple predator–prey pairs, not accounting for potentially more complex feeding behaviour of predators when multiple prey species or multiple predator individuals coexist (e.g. prey switching or interference competition). Second, our estimates of field energy fluxes assume that consumption rates increase linearly with prey abundances (encounter rates) (Emmerson *et al.* 2004; Neutel *et al.* 2007). Where handling and satiation lead to consumption saturation at high prey densities, we anticipate that energy fluxes should always saturate, rather than increase monotonically as prey body mass decreases (and thus prey abundance increases). Third, encounter rates may be influenced by body mass-related species traits such as the search area of the predator and the movement velocity of predator and prey (Aljetlawi *et al.* 2004). While these caveats may change some quantitative aspects of the model predictions (e.g. the continuous increase in total energy flux with decreasing prey body mass), qualitative differences among predictions of the metabolic and foraging models should be robust. Most importantly, this includes (1) the power-law (metabolic model) vs. hump-shaped (foraging model) relationship between per capita energy flux and predator body mass; and (2) the increase (metabolic model) vs. decrease (foraging model) in total energy flux with predator body mass. Future extensions of our approach will address how more complex foraging models that account for the caveats listed above may change the quantitative predictions of the models.

While metabolic theory accurately predicts physiological processes at the level of individuals (per capita metabolic demand and consumption) (Brown *et al.* 2004), it failed to accurately predict per link energy fluxes at high predator–prey body mass ratios. At these high ratios, energy fluxes were not driven by the predators' metabolic demand as assumed by metabolic theory. Instead, they depended primarily on behavioural aspects of the interaction, such as the prey's escape efficiency that increased with predator–prey body mass ratios (for $R > R_{max}$). Rooted in behavioural models of foraging theory, the hump-shaped foraging model successfully predicted the energy fluxes in the present study. Thus reconciling these two bodies of theory that successfully predict patterns at the level of individuals (metabolic theory) and links (foraging theory) will be an important step towards quantitative community ecology that predicts energy fluxes and abundances.

Interestingly, the predator–prey body mass ratios that characterize the maximum predation rates in our experiments are consistent with the average predator–prey body mass ratios found in natural food webs (Brose *et al.* 2006a). Consistent with prior studies (Wilson 1975; Wahlstrom *et al.* 2000; Bystrom *et al.* 2003; Aljetlawi *et al.* 2004; Finstad *et al.* 2006), our results suggest that predators may efficiently exploit prey that fall within a specific size range. Such a contiguous feeding range is also consistent with successful theoretical concepts of adaptive (Uchida, Drossel & Brose 2007) and static food web

topology (Williams & Martinez 2000; Loeuille & Loreau 2005; Stouffer, Camacho & Amaral 2006). Moreover, the foraging model predicts energy fluxes through individual feeding links, which offers a new perspective on the distribution of interaction strengths within food webs that ultimately drive network stability (Emmerson *et al.* 2004; Brose *et al.* 2006b; Montoya *et al.* 2006; Neutel *et al.* 2007). Specifically, our results suggest that the dominant per capita energy fluxes within a food web that are critically important for its stability (Bascompte *et al.* 2005; Neutel *et al.* 2007; Otto *et al.* 2007) occur between predator–prey pairs of intermediate body mass ratios (Fig. 3b). If our results generalize to other predator groups and ecosystem types, this approach allows predicting quantitative energy fluxes in natural food webs (Bersier, Banasek-Richter & Cattin 2002). Ultimately, we anticipate that this will enable a quantitative understanding of interaction strengths, energy fluxes and the stability of complex natural food webs.

References

Aljetlawi, A.A., Sparrevik, E. & Leonardsson, K. (2004) Prey–predator size-dependent functional response: derivation and rescaling to the real world. *Journal of Animal Ecology*, **73**, 239–252.

Bascompte, J., Melian, C.J. & Sala, E. (2005) Interaction strength combinations and the overfishing of a marine food web. *Proceedings of the National Academy of Sciences, USA*, **102**, 5443–5447.

Beckerman, A.P., Petchey, O.L. & Warren, P.H. (2006) Foraging biology predicts food web complexity. *Proceedings of the National Academy of Sciences, USA*, **103**, 13745–13749.

Berlow, E.L., Neutel, A.M., Cohen, J.E. *et al.* (2004) Interaction strengths in food webs: issues and opportunities. *Journal of Animal Ecology*, **73**, 585–598.

Bersier, L.F., Banasek-Richter, C. & Cattin, M.F. (2002) Quantitative descriptors of food-web matrices. *Ecology*, **83**, 2394–2407.

Brohmer, P. (2006) *Fauna von Deutschland*, 22nd edn Quelle & Meyer, Heidelberg, Germany.

Brose, U., Berlow, E.L. & Martinez, N.D. (2005) Scaling up keystone effects from simple to complex ecological networks. *Ecology Letters*, **8**, 1317–1325.

Brose, U., Jonsson, T., Berlow, E.L. *et al.* (2006a) Consumer–resource body-size relationships in natural food webs. *Ecology*, **87**, 2411–2417.

Brose, U., Williams, R.J. & Martinez, N.D. (2006b) Allometric scaling enhances stability in complex food webs. *Ecology Letters*, **9**, 1228–1236.

Brown, J.H., Gillooly, J.F., Allen, A.P., Savage, V.M. & West, G.B. (2004) Toward a metabolic theory of ecology. *Ecology*, **85**, 1771–1789.

Bystrom, P., Persson, L., Wahlstrom, E. & Westman, E. (2003) Size- and density-dependent habitat use in predators: consequences for habitat shifts in young fish. *Journal of Animal Ecology*, **72**, 156–168.

Carbone, C., Teacher, A. & Rowcliffe, J.M. (2007) The costs of carnivory. *PLoS Biology*, **5**, 363–368.

Emmerson, M.C. & Raffaelli, D. (2004) Predator–prey body size, interaction strength and the stability of a real food web. *Journal of Animal Ecology*, **73**, 399–409.

Emmerson, M., Montoya, J.M. & Woodward, G. (2005) Body size, interaction strength, and food web dynamics. *Dynamic Food Webs: Multispecies Assemblages, Ecosystem Development, and Environmental Change* (eds P. De Ruiter, J.C. Moore & V. Wolters), pp. 167–178. Elsevier/Academic Press, San Diego, CA, USA.

Finstad, A.G., Ugedal, O. & Berg, O.K. (2006) Growing large in a low grade environment: size dependent foraging gain and niche shifts to cannibalism in Arctic char. *Oikos*, **112**, 73–82.

Foelix, R.F. (1996) *Biology of Spiders*. 2nd edn. Oxford University Press, Oxford, UK.

Loeuille, N. & Loreau, M. (2005) Evolutionary emergence of size-structured food webs. *Proceedings of the National Academy of Sciences, USA*, **102**, 5761–5766.

McCann, K., Hastings, A. & Huxel, G.R. (1998) Weak trophic interactions and the balance of nature. *Nature*, **395**, 794–798.

Meehan, T.D. (2006) Energy use and animal abundance in litter and soil communities. *Ecology*, **87**, 1650–1658.

van der Meer, J. (2006) Metabolic theories in ecology. *Trends in Ecology and Evolution*, **21**, 136–140.

Montoya, J.M., Pimm, S.L. & Sole, R.V. (2006) Ecological networks and their fragility. *Nature*, **442**, 259–264.

Navarrete, S.A. & Berlow, E.L. (2006) Variable interaction strengths stabilize marine community pattern. *Ecology Letters*, **9**, 526–536.

Neutel, A.-M., Heesterbeek, J.A.P., van de Koppel, J. *et al.* (2007) Reconciling complexity with stability in naturally assembling food webs. *Nature*, **449**, 599–602.

Otto, S.B., Rall, B.C. & Brose, U. (2007) Allometric degree distributions facilitate food-web stability. *Nature*, **450**, 1226–1229.

Persson, L., Leonardsson, K., de Roos, A.M., Gyllenberg, M. & Christensen, B. (1998) Ontogenetic scaling of foraging rates and the dynamics of a size-structured consumer–resource model. *Theoretical Population Biology*, **54**, 270–293.

Peters, R.H. (1983) *The Ecological Implications of Body Size*. Cambridge University Press, New York.

Rall, B.C., Guill, C. & Brose, U. (2008) Food-web connectance and predator interference dampen the paradox of enrichment. *Oikos*, **117**, 202–213.

Reuman, D.C. & Cohen, J.E. (2005) Estimating relative energy fluxes using the food web, species abundance, and body size. *Advances in Ecological Research*, **36**, 137–182.

Scheu, S. (1992) Automated measurement of the respiratory response of soil microcompartments – active microbial biomass in earthworm feces. *Soil Biology and Biochemistry*, **24**, 1113–1118.

Schmitz, O.J. (2007) Predator diversity and trophic interactions. *Ecology*, **88**, 2415–2426.

Stouffer, D.B., Camacho, J. & Amaral, L.A.N. (2006) A robust measure of food web intervality. *Proceedings of the National Academy of Sciences, USA*, **103**, 19 015–19 020.

Uchida, S., Drossel, B. & Brose, U. (2007) The structure of food webs with adaptive behaviour. *Ecological Modelling*, **206**, 263–276.

Wahlstrom, E., Persson, L., Diehl, S. & Bystrom, P. (2000) Size-dependent foraging efficiency, cannibalism and zooplankton community structure. *Oecologia*, **123**, 138–148.

Weitz, J.S. & Levin, S.A. (2006) Size and scaling of predator–prey dynamics. *Ecology Letters*, **9**, 548–557.

Williams, R.J. & Martinez, N.D. (2000) Simple rules yield complex food webs. *Nature*, **404**, 180–183.

Williams, R.J. & Martinez, N.D. (2004) Stabilization of chaotic and non-permanent food web dynamics. *European Physical Journal of B*, **38**, 297–303.

Wilson, D.S. (1975) Adequacy of body size as a niche difference. *American Naturalist*, **109**, 769–784.

Wootton, J.T. & Emmerson, M. (2005) Measurement of interaction strength in nature. *Annual Review of Ecological Evolution Systems*, **36**, 419–444.

Yodzis, P. & Innes, S. (1992) Body size and consumer–resource dynamics. *American Naturalist*, **139**, 1151–1175.